Materials Today Communications 8 (2016) 196–204

Contents lists available at ScienceDirect

Materials Today Communications

journal homepage: www.elsevier.com/locate/mtcomm

Carbon nanotubes and nanofibers as strain and damage sensors for smart cement

Panagiota T. Dalla, Konstantinos G. Dassios*, Ilias K. Tragazikis, Dimitrios A. Exarchos, Theodore E. Matikas

Department of Materials Science and Engineering, University of Ioannina, Dourouti University Campus, Ioannina GR-45110, Greece

ARTICLE INFO

Article history:
Received 3 June 2016
Received in revised form 22 June 2016
Accepted 27 July 2016
Available online 28 July 2016

Keywords:
Carbon nanotubes
Carbon nanofibers
Smart cement
Electrical properites
Percolation theory
Damage sensing
Strain sensing

ABSTRACT

The present paper reports on the strain and damage sensing potential of carbon nanotubes and carbon nanofibers embedded in cement mortars. Prismatic and three-point bending specimens were prepared at various nano-inclusion concentrations for measurement of the material's surface electrical resistivity, establishment of its electrical percolation threshold, assessment of its piezoresistive response under cyclic compressive loading and for damage detection under pure bending of the mortars. Percolation theory conditions were met at a tube concentration of ca. 0.6% by weight of cement while both nanotubes and nanofibers endowed smartness to the mortars which exhibited remarkable electrical sensitivity to applied load, with fully-recoverable electrical resistances varying in an inverse relation with compressive stress. The potential of nanotubes and nanofibers as damage sensors in percolated mortars was manifestedby dramatic increases of in situ electrical resistivity under three-point bending testing, at loading instances as early as the maximum load, hence providing timely failure warnings. Differences in the strain and damage sensing potentials of the two types of nano-inclusions is presented and discussed in the text.

1. Introduction

Electrical conductivity, the property which quantifies how strongly the material assists electric current transport, is currently the most desirable characteristic of next-generation smart cement-based materials. The property is often expressed by means of its inverse, electrical resistivity, which can attain values ranging from 10^{-6} Ohm cm for highly conductive metals, to 10^{19} Ohm cm for highly insulating rubber and certain polymers. As a porous material, concrete exhibits a wide range of resistivities depending mainly on moisture content [1], temperature [2], cement type, water-to-cement ratio and amount and type of aggregates, admixtures and supplementaries in the raw materials [3].

Electrical resistivity is extremely significant for a variety of cement-based applications such as concrete railway ties on long-line railroads, transit lines, hospital operating room floors and cathodic protection systems [4]. Moreover, electrical resistivity measurements as non-invasive methodologies, have been suggested for assessment of the effect of re-alkalisation of carbonated concrete [5], monitoring the health of carbon fiber-reinforced concrete [6,7], and monitoring water, ionic penetration and moisture displacement within the materials [8–15]. Electrical resistivity measurements have also been suggested for assessing microstructural alterations in hydrating cement-based materials [16]. Elastic waves and electrical resistivity measurements were used by Kang et al. for studying the effect of the freezing-thawing process on sand-silt mixtures [17].

Carbon nanotubes (CNT), the one-dimensional allotropes of carbon considered as one of the most remarkable materials of the 21st century, are particularly efficient in endowing electrical transport potential to low-conductivity matter such as cement [18,19]. With average diameters as low as 1.2 nm the tubes can be conducting or semiconducting by adjustment of the imposed electrical field [19]. CNTs have attracted extensive scientific attention due to their remarkable physical, mechanical and electrical properties. Not long after the announcement of some unique CNT applications such as electrically conducting polymer composites, field emission electron sources for flat panel displays, hydrogen storage media in electric vehicles or laptop computers and microwave generators [20–24], the tubes demonstrated potential also in cement-based materials to which they can endow multi-functional characteristics such as enhanced electrical and thermal transport properties while simultaneously acting as nano-reinforcement to the mechanical behavior [19]. In smart cements, the tubes can act as internal self-

* Corresponding author.
E-mail address: kdassios@cc.uoi.gr (K.G. Dassios).

http://dx.doi.org/10.1016/j.mtcomm.2016.07.004
2352-4928/

monitoring sensors for inner defects hence eliminating the need for embedded, attached or remote sensing systems [25]. The sensing ability of cement-based composites was firstly documented by Han et al. [26] and is associated with their piezoresistive effect, i.e. the change in their electrical resistance under external mechanical stimulus. The piezoresistive behavior of nano-modified cement stems from the variation, due to external loading -usually of compressive nature- in the contact resistance between the electrically conducting nano-inclusions and the bulk cement-based material [27].

Efficient improvement of the electrical transport properties of cement by embedded carbon nanotubes requires that percolation theory conditions are satisfied. Therein, establishment of a critical nanotube concentration is required for adjacent nano-inclusions to critically contact one another so that a continuous, electrically conductive path is formed throughout the material which leads to a sudden dramatic decrease in resistivity. The tube concentration where such conditions are met is known as the electrical percolation threshold of the given material system [27]. At the threshold, the curve of resistivity versus inclusion concentration renders S-shaped [27]. The percolation effect has been studied in great extent for CNT-loaded polymers however extremely limited information is available for cement-based materials [27–29]. Ambrosetti et al. [30] studied theoretically and numerically the percolation of electrical properties of carbon nanotube composites.

Measurement of the in-plane electrical resistance of cement-based materials in situ during testing can reveal the damage state of the materials due to either damage infliction (and corresponding subsequent opening of microcracks) or healing by microcrack closing [31]. For example, Bontea et al. monitored damage in short carbon fiber-reinforced concrete by measurement of DC electrical resistance and found that resistance decreased during compression and increased upon damage development [32]. In this manner the strain/stress state during dynamic loading could be related to the origin of the damage.

Electrical resistivity measurements in cement-based materials are typically conducted by one-, two- or four-probe methods. The latter, also called Wenner method [33], is considered as the most accurate; it uses four electrodes fixed onto the concrete surface and the current is applied to the two outer electrodes while the two inner ones measure the difference in potential. In the case of homogeneous materials like concrete, an additional factor, K, accounting for probe spacing, specimen dimensions and temperature must also be taken into consideration in calculation of the resistivity as suggested by Morris et al. [34]. Resistivity data from cylindrical and prismatic specimens also require correction as suggested in [35]. Coppola et al. [36] and Cao et al. [37] recently demonstrated the effectiveness of the four-point method in monitoring stress in CNT-loaded cement and in assessing the steel fiber dispersion in cement mortars, respectively.

The main objective of the present paper is to investigate the strain and damage sensing capabilities of two types of carbon nano-inclusions, namely carbon nanotubes and carbon nanofibers, in imparting smartness to cement. For this task, a series of nano-modified cement mortars were prepared at varying nanotube and nanofiber loadings and their electrical transport performance was examined in terms of surface electrical resistivity measurements for establishment of the percolation threshold, piezoresistivity measurements under cyclic loading for assessing the strain sensing capacity of the nano-inclusions and bending tests for establishment of their potential as instant damage sensors and early warning indicators.

Table 1
Properties of multi-wall carbon nanotubes.

Parameter	Value
Length range	5–15 μm
Diameter range	20–40 nm
Synthesis method	catalytic CVD
Purity	≥95%
Ash	≤0.2 wt.%
Specific surface area	40–300 m^3/g
Amorphous carbon content	≤3%

Table 2
Properties of carbon nanofibers.

Parameter	Value
Length	20–200 μm
Average diameter	100 nm
Average pore volume	0.12 cm^3/g
Purity	≥98%
Molecular Weight	12 g/mol
Iron content	<14,000 ppm

2. Experimental procedure

2.1. Materials

Five cement mixtures, each with different CNT loading, were prepared according to standard protocol "BS EN 196-1" intended for measurement of surface electrical resistivity. Sets of six prismatic specimens, dimensions of $40 \times 40 \times 160\ mm^3$ were fabricated for each mixture/loading value. Mixtures contained ordinary Portland cement type "I 42.5t", regular tap water, natural sand, long multi-wall carbon nanotubes commercially available by Shenzhen Nanotech Port Co. Ltd. (Shenzhen, China) and Viscocrete Ultra 600 superplastisizer (Sika AG, Baar, Switzerland) as CNT dispersant agent, in a 1:1 weight ratio to CNT. The specific superplastisizer is a native concrete additive which proved highly effective for CNT dispersion and rendered employment of conventional dispersion methods, such as surfactant use and chemical tube functionalization, unnecessary [38]. The main properties of the nanotubes used in this study are given in Table 1. Water to cement ratio was maintained at 0.5 while the tubes were added at varying concentrations of 0.2, 0.4, 0.6 and 0.8%, by weight of cement and a reference mixture without nano-inclusions was prepared.

For piezoresistivity measurements under three-point bending tests and for monitoring damage, six additional prismatic specimens, same dimensions as before, were fabricated at a tube loading of 0.6 wt.% of cement. The particular loading value was selected following the surface electrical resistivity measurements according to the rationale presented in Section 3.3. The initial notch of the bending specimens was 20 mm and crack opening displacement was measured using an external clip-on digital extensometer. External electrical contacts were prepared by direct embedment in the fresh mortars of four stainless steel grids, dimensions of $50 \times 20 \times 1\ mm^3$, immediately after the mortars were poured in the molds. The grids were embedded 30 mm deep into the samples to ensure good contact of the electrodes to the sensed material over a large, statistically representative material volume. The two inner probes (used for voltage measurement) were positioned symmetrically at a distance of 40 mm while the outer (used for passing current) at a 60 mm distance (Fig. 1). Two additional mixtures were prepared with carbon nanofibers as nano-inclusions at loadings of 0.2 and 0.6% by weight of cement. The particular mixtures were produced following the same protocol with CNT-based mixtures while the properties of the nanofibers used are shown in Table 2.

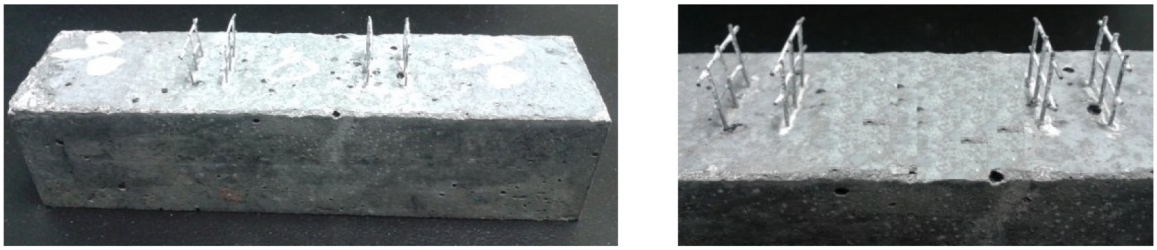

Fig. 1. Embedded electrode configuration in the CNT/cement prismatic mortars.

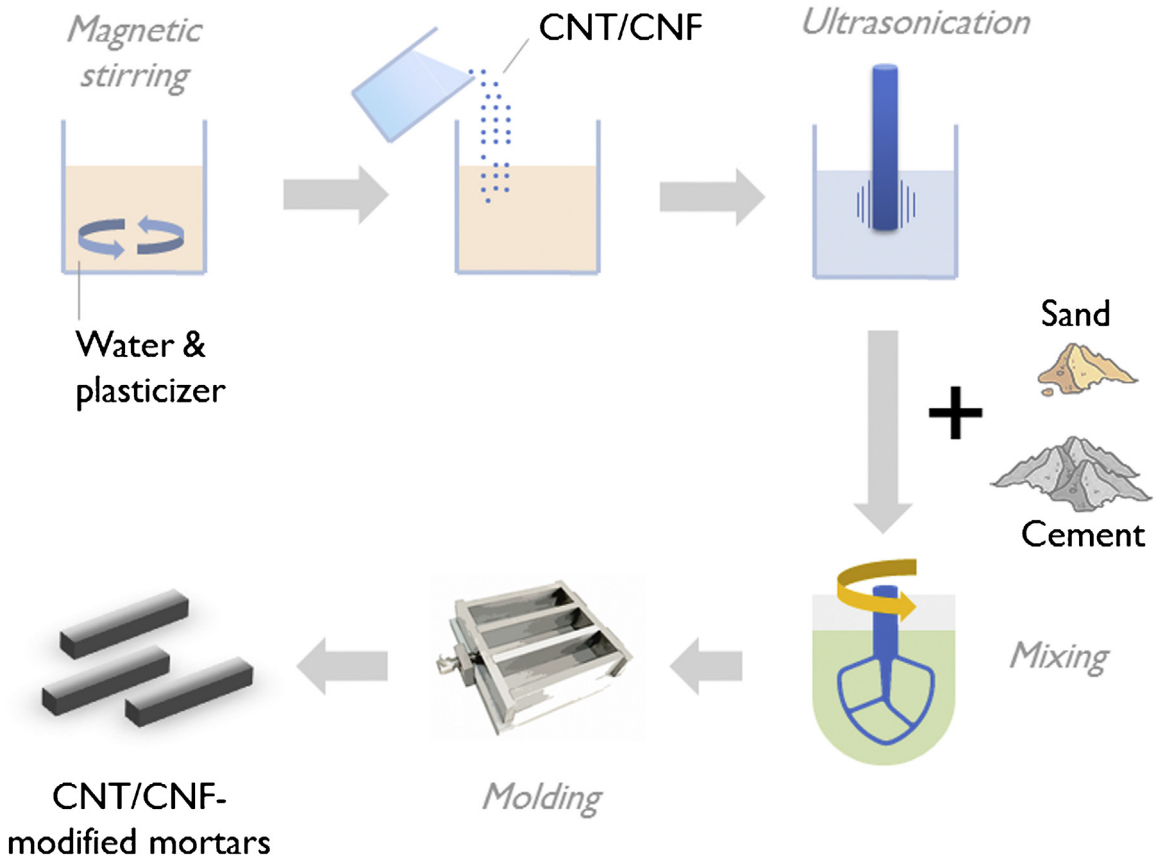

Fig. 2. Schematic representation of the nano-modified mortars manufacturing process.

2.2. Preparation of nanomodified mortars

The experimental procedure for the preparation of CNT- and CNF-modified cemenmortarts is illustrated in Fig. 2 and consisted of three main steps. Initially, suspensions were produced by mixing tap water and the plasticizer for 2 min using magnetic stirring. Subsequently, the nanophase, CNT or CNF, was added to the solution and the resulting suspension was ultrasonicated for 30 min in room temperature at an abiding power. Ultrasonication parameters were established following a tedious analysis which involved laser diffractometry measurements of CNT agglomerate analysis [39]. Finally, the cement and sand suspensions were mixed in a rotary mixer with a flat beater for a total of 4 min in low and high speeds successively, as per the requirements of BS EN 196-1 standard. Immediately after mixing, the fresh mortar was poured into oiled steel moulds of inner dimensions of $40 \times 40 \times 160\,mm^3$ and was let to rest for 24 h before demolding. Specimens were placed into a 100% humidity room for 28 days before being dried in an oven at 60 °C for three days and then at 90 °C for another two days, for elimination of the polarization effect.

2.3. Experimental methods

2.3.1. DC surface electrical resistivity measurements

The effect of nanotubes on the surface electrical resistivity of cement mortars was investigated through DC electrical measurements conducted using a custom-built contact electrical resistivity probe connected to an ultra-high precision digital electrometer/high resistance meter (Keithley 6517B, Tektronix Inc., Beaverton, Oregon, USA) capable of measuring resistances up to $10^{18}\,\Omega$ with a 10×10^{18} A current measurement resolution, as shown in Fig. 3. The probe consisted of a circular head comprised of 22 concentrically-arranged spring-loaded pin electrodes with conductive rubber ends for optimal contact with the non-planar cement surfaces. The head rested on a z-translational stage which could be lowered and brought into contact with the specimen at constant force by means of a lever (Fig. 3b and c). Mortar specimens were placed on the base plate of the apparatus on top of an insulating sheet to avoid current leakage.

Surface resistivity was determined according to Ohm's law, by measuring the current as a result of application of a voltage poten-

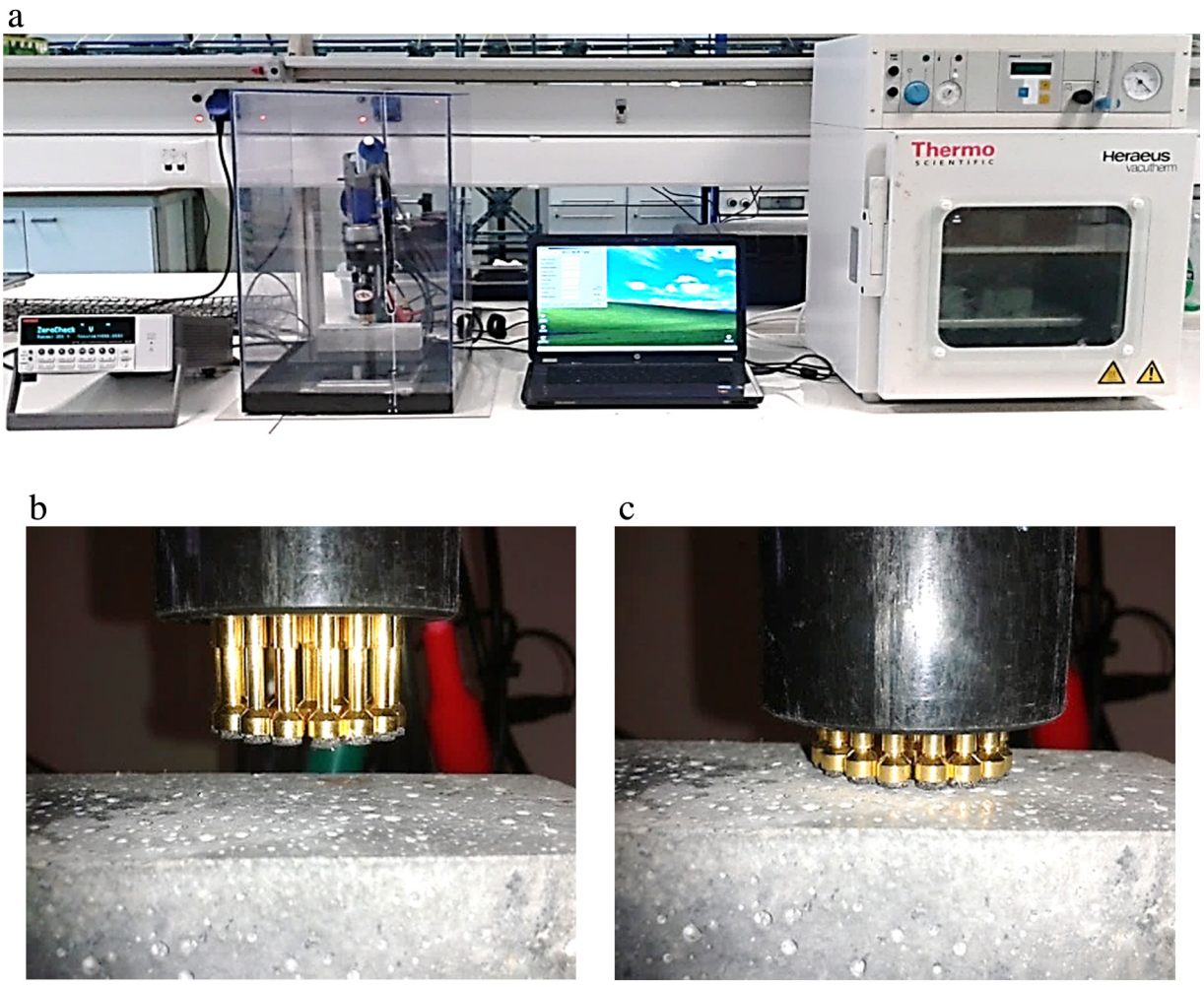

Fig. 3. (a) Apparatus line-up for surface resistivity measurements. (b and c) Sample and probe before and during resistivity measurement.

tial across the surface of the sample. Six specimens were tested at each nano-inclusion composition. Fig. 4 illustrates the two types of electrical resistivity data collected: i) electrical current in amperes as a function of test time in seconds and ii) surface resistivity in Ohms per square as a function of readings count at the indicated voltage. The resistivity value in each specimen was established as the average of eight consecutive readings.

2.3.2. Piezoresistive behavior

The piezoresistive behavior of nano-modified mortars was assessed by measurement of their electrical response during cyclic compressive loading of a maximum load of 2 kN in the direction perpendicular to the embedded electrodes. The tests were performed at a load rate of 0.025 MPa/s on an Instron 8800 servo-hydraulic frame (Illinois Tool Works, Glenview, IL, USA), as shown in Fig. 5. Each unloading-reloading cycle had a duration of approximately 100 s and a total of six cycles were applied to each specimen. During cyclic loading, the electric current of the specimens under an applied voltage of 30 V was recorded. The change in DC electrical resistance was calculated as $(R\text{-}R_0)/R_0$, where R is the instant electrical resistance on the loaded specimen and R_0 is the initial electrical resistance prior to load application.

2.3.3. Damage detection under three point bending

Damage and crack formation and propagation in the mortars during loading lead to the collapse of the electrically conductive network, hence also to resistivity increases. Three point bending tests were performed with simultaneous electrical resistance measurements using the four-probe method as shown in Fig. 6. The tests were performed under crosshead displacement control at a speed of 0.01 mm/s while an applied voltage of 30 V was used.

3. Results and discussion

3.1. DC electrical resistivity measurements

The primer task of the current study was the establishment of the relation between carbon nanotube loading and room temperature DC surface electrical resistivity of nano-modified cement mortars. Average values and standard deviation of resistivity obtained for each mixture is plotted as a function of tube loading in the corresponding mixture, in Fig. 7. The observed behavior manifests a dramatic effect of CNT presence on surface electrical resistivity of the nano-modified mortars with property values decreasing by approximately three orders of magnitude from the control value (plain specimens) as tube concentration increases from 0.4 to 0.6 wt.%. This finding suggests that a CNT loading of 0.6 wt.% of cement is the percolation threshold for the material system under investigation as it allows a remarkably faster electrical current flow of ions through the material by establishment of a continuous conductive network of carbon nanotubes throughout its volume.

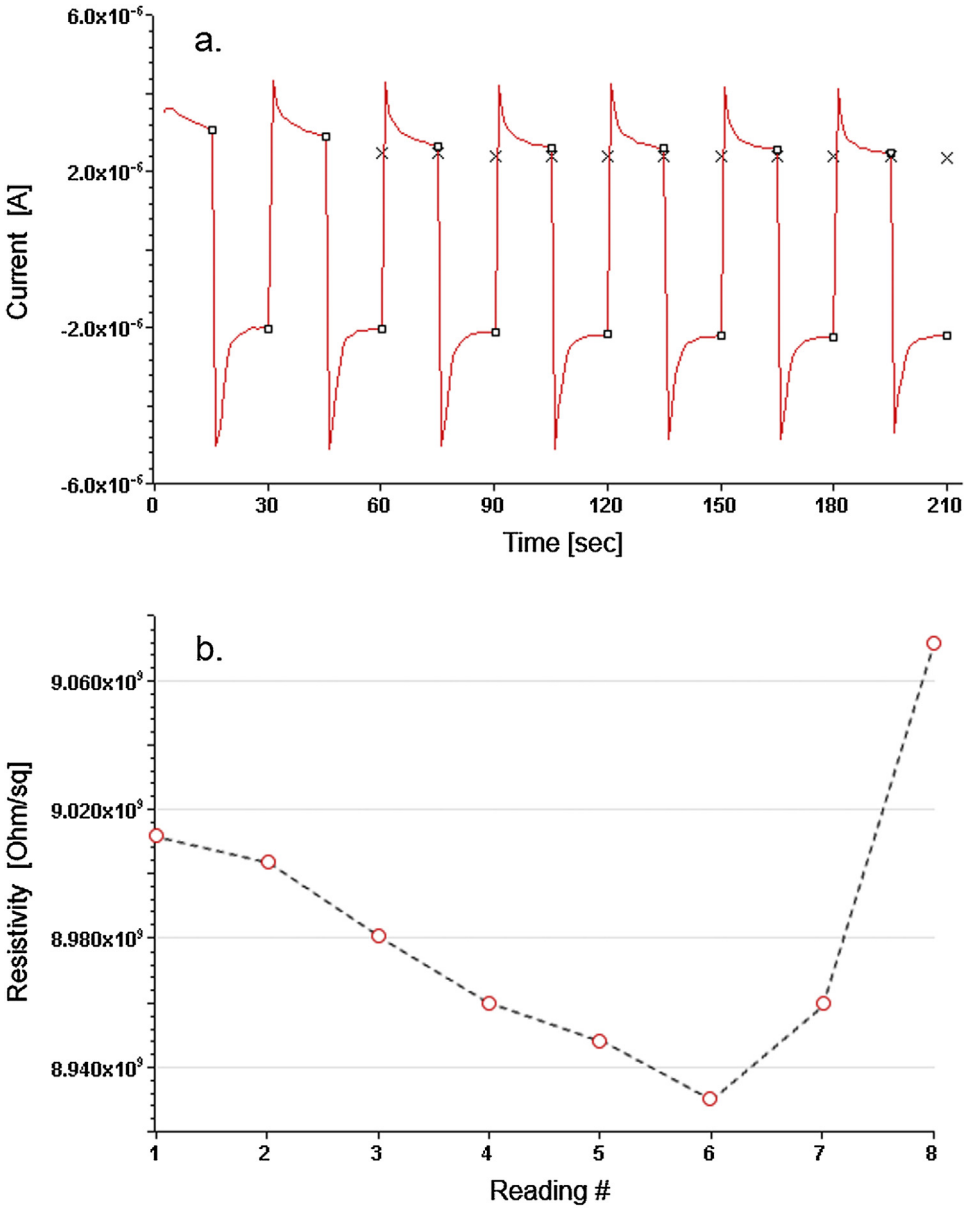

Fig. 4. Types of data collected during electrical resistivity measurements. (a) Current vs time and (b) Resistivity vs readings count.

3.2. *Piezoresistivity effect-strain sensing*

The fractional change in electrical resistance of a mortar modified with 0.6% wt. of cement carbon nanotubes, just above the percolation threshold, is plotted as a function of cyclic compressive loading duration, for all six applied cycles, in Fig. 8. For ease of conception of instantaneous stress level, compressive stress is also included as a right hand side y-axis. The compressive loading amplitude of 2 kN corresponds to a maximum compressive stress amplitude of 1.25 MPa for the specimens under investigation. It is observed that electrical resistance values maintain a negative sign throughout testing while the property decreases during the loading stage and increases upon unloading. The behavior depicted in Fig. 8 manifests that the change in resistance invoked in each unloading/reloading cycle is fully reversible, as the previous resistance level is completely recovered in the following cycle. This particular characteristic is important in that it validates nanotubes as strain sensors with a remarkable sensitivity to external loading, hence imparting "smartness" to the material. The observed behavior can be explained upon the level of compaction caused to the specimen during compressive loading which facilitates physical contact of the electrically conductive tubes and easier current flow. The opposite phenomenon occurs during unloading which causes electrical resistance to increase.

Fig. 9 illustrates the fractional change in electrical resistance, under the same loading protocol as the previous case, for mortars modified with 0.2 and 0.6 wt.% of cement carbon nanofibers. A similar behavior as with nanotubes is observed, with fully-recoverable electrical resistances varying in an inverse relation to applied compressive stress. However, the smaller resistance change amplitudes observed, manifest a lower strain sensing ability of CNFs compared to CNTs under similar loading conditions. This is not unlinked to the difference in dimensions of CNFs, both in length as well as in diameter, compared to the CNTs employed in this study (Tables 1 and 2). Longer and bigger nano-inclusions such as nanofibers facilitate physical contact hence increase the probability of formation of a conductive path at lower inclusion concentrations.

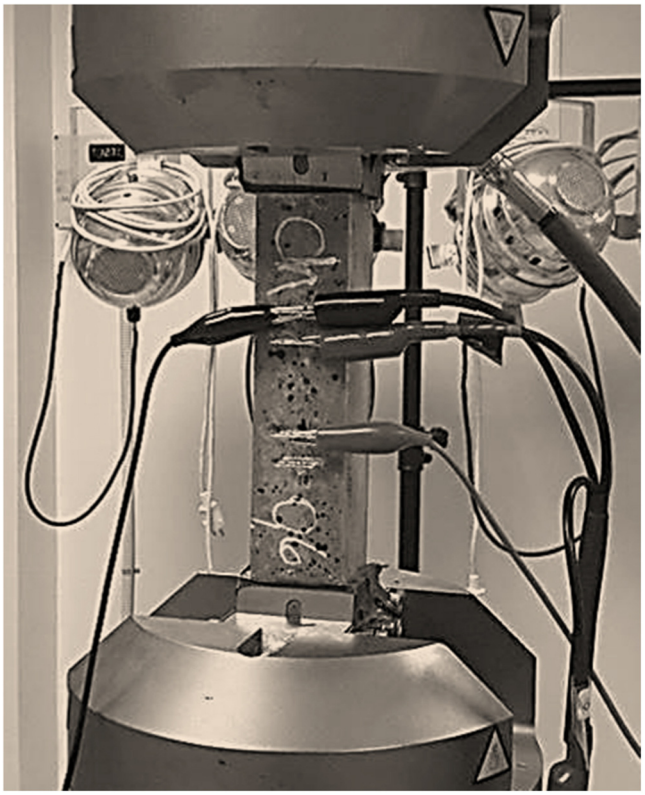

Fig. 5. Nano-modified mortar undergoing cycling loading with simultaneous piezoresistivity measurement.

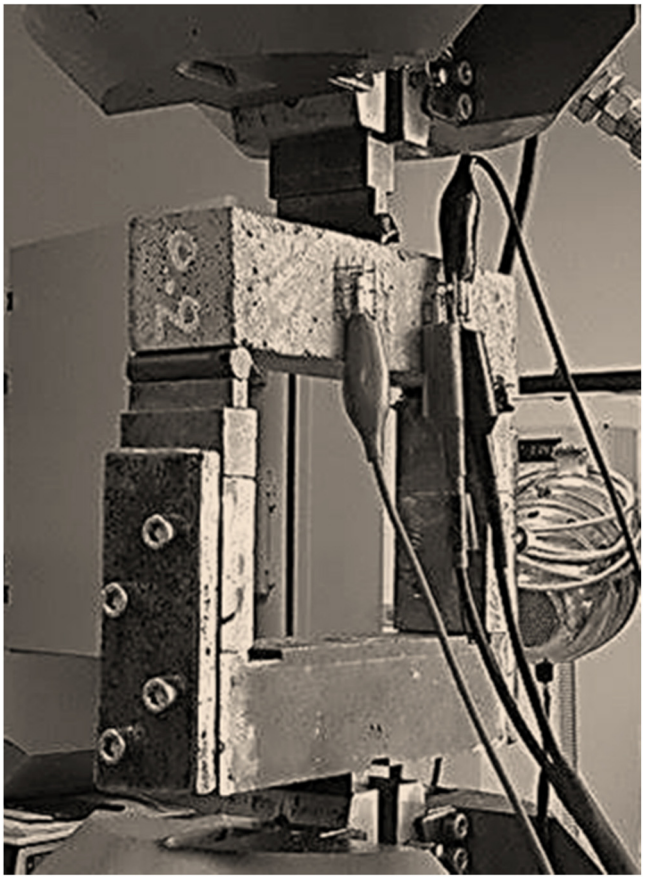

Fig. 6. Nano-modified mortar during three point bending testing with simultaneous electrical resistivity measurement.

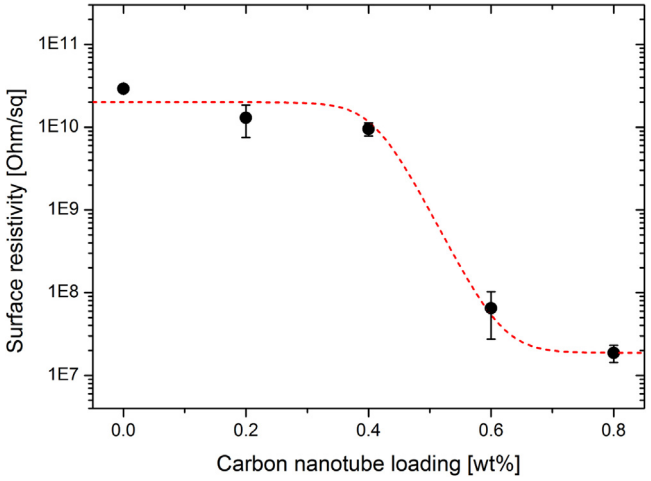

Fig. 7. Average surface electrical resistivity as a function of CNT loading in the nano-modified mortars.

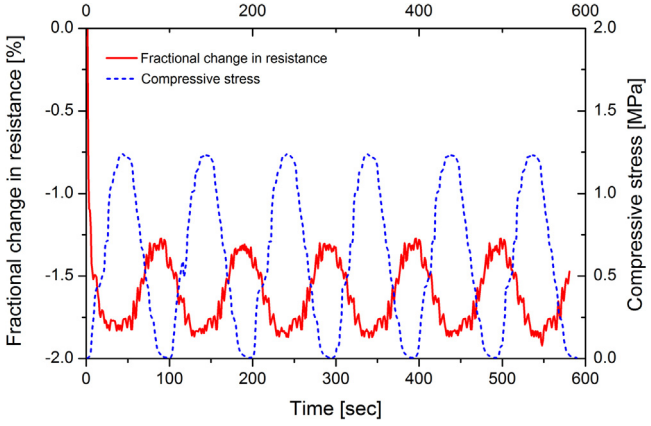

Fig. 8. Fractional change in electrical resistance under compressive cyclic loading in a mortar loaded with 0.6 wt.% of cement CNT.

Table 3
Average change in electrical resistance for mortars modified with different loadings of CNT and CNF.

Type	Concentration [wt.% of cement]	Average change in electrical resistance [%]
Carbon nanotubes	0.6	1.8
Carbon nanofibers	0.2	1.64
Carbon nanofibers	0.6	0.95

Table 3 summarizes the average change of electrical resistance in mortars modified with different concentrations of CNTs and CNFs. The change in mortars with 0.6 wt.% CNTs is 1.8%, a value which decreases by almost 50% when the same concentration of CNFs is used. This does not necessarily signify that CNFs are less effective in endowing sensing capability to cement than nanotubes. On the opposite, it implies that a CNFs concentration of only 0.2 wt.% of cement is sufficient to provide the mortar with the average resistivity provided by 0.6% CNTs. Hence, in terms of electrical resistance, smaller concentrations of CNFs may provide similar results as higher concentrations of nanotubes.

It is worth recalling that the amount of nano-reinforcement directly influences the conductive network inside the mortars. When the concentration level is extremely low, the thickness of the insulating matrix between the adjacent nanotubes is large and the possibility of formation of a conductive path under external loading is small. The increase of nano-inclusion concentration, results

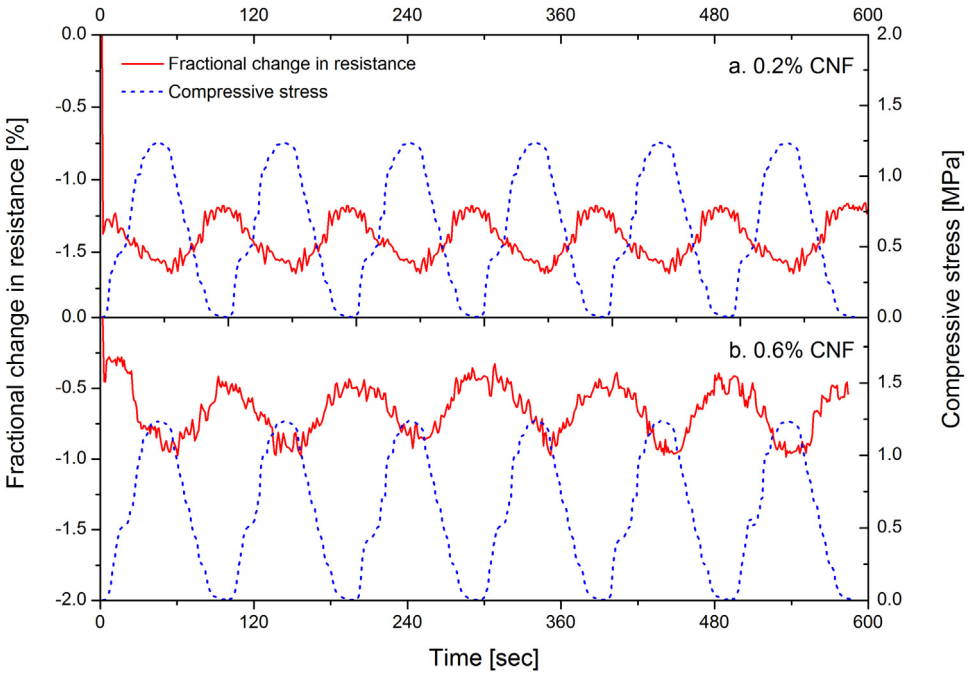

Fig. 9. Fractional change in electrical resistance under cyclic compressive stress for mortars with 0.2 (a) and 0.6 wt.% of cement, CNF (b).

in the decrease of the thickness of the insulating matrix between adjacent nanotubes hence also in current flow facilitation through the material. Increase of the nano-inclusion concentration above the threshold does not further improve the flow as the conductive network stabilizes and does not change significantly under exterior loading.

3.3. *Damage sensing under bending*

Selection of mortars with 0.6 wt.% of cement CNTs for three-point bending testing was based on the electrical percolation threshold established in Section 3.1. Fig. 10 depicts the typical change in electrical resistance measured in situ during three point bending; the load-displacement behavior of the mortar is also included in the graph for ease of conception of the instant loading level. Based on the trend of the electrical resistance curve, the material's response can be categorized into three main regimes. The first is the elastic regime which extends up to the attainment of maximum load at a displacement of 0.022 mm and involves small increases in resistance. The second regime occupies a narrow displacement range within 0.022–0.03 mm wherein a dramatic monotonic increase in electrical resistance, of approximately one order of magnitude, takes place. The mechanical response of the material within this regime is a smooth load drop after the maximum load typically linked to multiple crack formation and propagation. The final regime extends from the displacement of 0.03 mm up to ultimate failure and involves a small to negligible increase in resistance attributed to merging of multiple crack paths and complete collapse of the conductive network. The succession of the three regimes demonstrates a remarkable damage sensing potential of the embedded nanotubes wherein a sudden increase in electrical resistance can provide early warnings of upcoming material catastrophe.

Fig. 11 shows the corresponding change in electrical resistance along with instantaneous three-point bending response, for mortars modified with carbon nanofibers at 0.2 and 0.6 wt.% of cement, respectively. Comparably to CNT-modified mortars, a dramatic increase in electrical resistance is also found linked to the

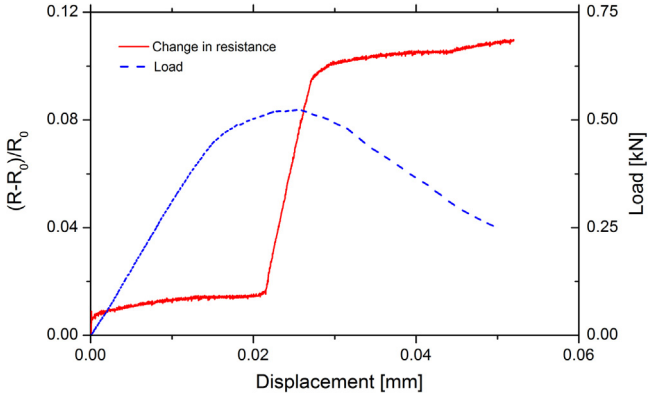

Fig. 10. Change in electrical resistance under crosshead displacement control three point bending in a mortar with 0.6 wt.% of cement CNT.

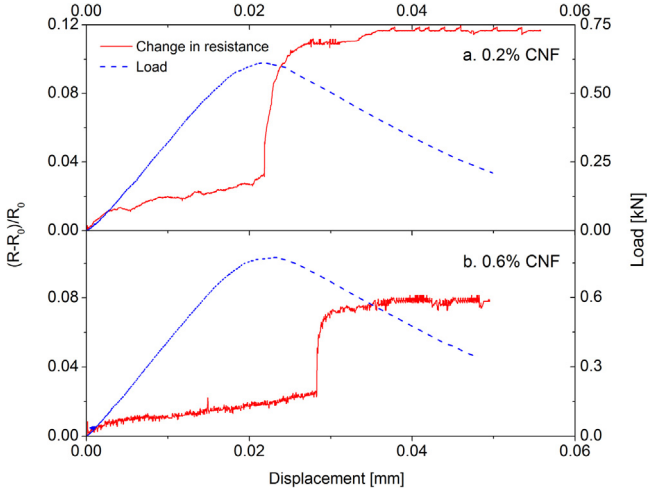

Fig. 11. Change in electrical resistance under crosshead displacement control three point bending in mortar with 0.2 (a) and 0.6% wt. of cement CNF (b).

attainment of the maximum load capacity of the materials hence predicting the onset of catastrophic damage leading to ultimate failure. It is nonetheless relevant to note that the resistance jump is smaller in mortars modified with 0.6 wt.% CNFs than both in those with 0.2% CNFs and in those with 0.6 wt.% CNTs. Common to the piezoresistivity results, this effect is directly associated with the dimensions of the nano-phase; therein CNFs, longer and thicker than CNTs, are capable of forming conductive/percolated networks at lower concentrations that the latter. For the same reason, reference conductivity values are higher in mortars with high CNF concentrations and this limits the evidenced conductivity jump at the maximum load. Although the sensing behavior depicted in Figs 10 and 11 is not dissimilar to that offered by other types of conducting inclusions for mortars, it must be recalled that the damage sensing potential reported herein is achieved at a nano-inclusion concentration of only 0.6 wt.% of cement, which is a fraction of the typically required conductive filler concentrations. Moreover, recent results with the same type of nanotubes demonstrate their high effectiveness in improving the flexural response of the mortars [38].

4. Conclusions

Cement mortars modified by two types of nano-inclusions, namely carbon nanotubes and carbon nanofibers were prepared and their strain and damage sensing potentials in the development of next generation smart cements was investigated. Surface electrical resistivity was measured on standard prismatic specimens with varying concentrations of carbon nanotubes using a novel custom-built multi-electrode probe connected to an ultra-high precision electrometer and the electrical percolation threshold was established at a CNT concentration of 0.6% by weight of cement in the mortars. CNT- and CNF-modified mortars were tested in cyclic compression with simultaneous four-point electrical resistivity measurements made possible by embedment of metallic grids during the production phases. The mortars exhibited remarkable piezoresistance characteristics with fully-recoverable electrical resistances at the end of each cycle which varied in an inverse relation to applied stress due to the instant compaction level. Three-point bending tests revealed the remarkable damage sensing capability of embedded nano-inclusions evidenced by dramatic resistivity jumps at loading levels as early as the maximum load, hence providing valuable warning signs and considerable time window for reaction. Variations in the strain and damage sensing potential of nanotubes and nanofibers in rationalized upon the dimensional differences of the two types of nano-inclusion types.

Aknowledgments

This research project has been co-financed by the European Union (European Regional Development Fund – ERDF) and Greek national funds (General Secretariat for Research and Technology) through the Operational Program "Competitiveness and Entrepreneurship and Regions in Transition" of the National Strategic Reference Framework (NSRF 2007–2013), under the program "Cooperation 2011, Partnerships of Production and Research Institutions in Focused Research and Technology Sectors".

References

[1] D.A. Whiting, M.A. Nagi, Electrical Resistivity of Concrete—A Literature Review, Portland Cement Association, Skokie, Illinois, USA, 2016.
[2] O. Sengul, Use of electrical resistivity as an indicator for durability, Constr. Build. Mater. 73 (2014) 434–441.
[3] F. Rajabipour, J. Weiss, Electrical conductivity of drying cement paste, Mater. Struct. 40 (10) (2007) 1143–1160.
[4] A.N. Hanna, Concrete ties for U.S. railroads -an update, in: D.R. Morgan (Ed.), SP-93: Concrete in Transportation, American Concrete Institute (ACI), 1986, pp. 267–286, Document: SP93-13.
[5] W. Yeih, J.J. Chang, A study on the efficiency of electrochemical realkalisation of carbonated concrete, Constr. Build. Mater. 19 (7) (2005) 516–524.
[6] M. Chiarello, R. Zinno, Electrical conductivity of self-monitoring CFRC, Cem. Concr. Compos. 27 (4) (2005) 463–469.
[7] J. Cao, D.D.L. Chung, Electric polarization and depolarization in cement-based materials studied by apparent electrical resistance measurement, Cem. Concr. Res. 34 (3) (2004) 481–485.
[8] W.J. McCarter, G. Starrs, T.M. Chrisp, Electrical conductivity diffusion, and permeability of Portland cement-based mortars, Cem. Concr. Res. 30 (9) (2000) 1395–1400.
[9] W.J. McCarter, H. Ezirim, M. Emerson, Properties of concrete in the cover zone: water penetration sorptivity and ionic ingress, Mag. Concr. Res. 48 (176) (1996) 149–156.
[10] W. McCarter, Monitoring the influence of water and ionic ingress on cover-zone concrete subjected to repeated absorption, Cem. Concr. Aggregates 18 (1) (1996) 55–69.
[11] W.J. Weiss, J.D. Shane, A. Mieses, T.O. Mason, S.P. Shah, Aspects of monitoring moisture changes using electrical impedance spectroscopy, in: Proceedings of the 2nd Symposium on Self-Desiccation and Its Importance in Concrete Technology, Lund, Sweden, 1999.
[12] A. Schiebl, W.J. Weiss, J.D. Shane, N.S. Berke, T.O. Mason, S.P. Shah, Assessing the moisture profile of drying concrete using impedance spectroscopy, Concr. Sci. Eng. 2 (6) (2000) 106–116.
[13] W.W.F. Rajabipour, J.D. Shane, T.O. Mason, S.P. Shah, Procedure to interpret electrical conductivity measurements in cover concrete during rewetting, J. Mater. Civ. Eng. 17 (5) (2005) 586–594.
[14] T. Schmit, F. Rajabipour, W.J. Weiss, Investigating the Use of a Diffuse Measurement Interpretation for Analyzing in Situ Electrical Measurements, Conference Proceedings, Vancouver, Canada, 2005.
[15] H. Li, H. Xiao, J. Ou, Effect of moisture on electrical properties of carbon black-filled cement composites, american concrete institute, ACI Spec. Publ. 254 (2008) 133–144.
[16] B.J. Christensen, T. Coverdale, R.A. Olson, S.J. Ford, E.J. Garboczi, H.M. Jennings, T.O. Mason, Impedance spectroscopy of hydrating cement-based materials: measurement interpretation, and application, J. Am. Ceram. Soc. 77 (11) (1994) 2789–2804.
[17] M. Kang, J.S. Lee, Evaluation of the freezing–thawing effect in sand–silt mixtures using elastic waves and electrical resistivity, Cold Reg. Sci. Technol. 113 (2015) 1–11.
[18] S. Iijima, Helical microtubules of graphitic carbon, Nature 354 (6348) (1991) 56–58.
[19] R. Siddique, A. Mehta, Effect of carbon nanotubes on properties of cement mortars, Constr. Build. Mater. 50 (2014) 116–129.
[20] A.G. Rinzler, J.H. Hafner, P. Nikolaev, L. Lou, Unraveling nanotubes: field emission from an atomic wire, Science 269 (5230) (1995) 1550–1553.
[21] N.S. Lee, D.S. Chung, I.T. Han, et al., Application of carbon nanotubes to field emission displays, Diamond Relat. Mater. 10 (2) (2001) 265–270.
[22] R. Rosen, W. Simendinger, C. Debbault, H. Shimoda, L. Fleming, B. Stoner, O. Zhou, Application of carbon nanotubes as electrodes in gas discharge tubes, Appl. Phys. Lett. 76 (13) (2000) 1668–1670.
[23] H. Sugie, M. Tanemura, V. Filip, K. Iwata, K. Takahashi, F. Okuyama, Carbon nanotubes as electron source in an x-ray tube, Appl. Phys. Lett. 78 (17) (2001) 2578–2580.
[24] R.H. Baughman, A.A. Zakhidov, W.A. Heer, Carbon nanotubes-the route toward applications, Science 297 (5582) (2002) 787–792.
[25] S.P. Wu, X.M. Liu, Q.S. Ye, L.I. Ning, Self-monitoring electrically conductive asphalt-based composite containing carbon fillers, Trans. Nonferrous Met. Soc. China 16 (2006) 512–516.
[26] B. Han, G. Qiao, H. Jiang, Piezoresistive response extraction for smart cement-based composites/sensors, J. Wuhan Univ. Technol. Mater. Sci. Ed. 27 (4) (2012) 754–757.
[27] S. Wen, D.D.L. Chung, Double percolation in the electrical conduction in carbon fiber reinforced cement-based materials, Carbon 45 (2) (2007) 263–267.
[28] N. Xie, X. Shi, D. Feng, B. Kuang, H. Li, Percolation backbone structure analysis in electrically conductive carbon fiber reinforced cement composites, Compos. Part B: Eng. 43 (8) (2012) 3270–3275.
[29] S.H. Foulger, Electrical properties of composites in the vicinity of the percolation threshold, J. Appl. Polym. Sci. 72 (12) (1999) 1573–1582.
[30] G. Ambrosetti, C. Grimaldi, I. Balberg, T. Maeder, A. Danani, P. Ryser, Solution of the tunneling-percolation problem in the nanocomposite regime, Phys. Rev. B 81 (15) (2010) 155434.
[31] S. Wen, D.D.L. Chung, Damage monitoring of cement paste by electrical resistance measurement, Cem. Concr. Res. 30 (12) (2000) 1979–1982.
[32] D.-M. Bontea, D.D.L. Chung, G.C. Lee, Damage in carbon fiber-reinforced concrete monitored by electrical resistance measurement, Cem. Concr. Res. 30 (4) (2000) 651–659.
[33] J.F. Lataste, M. Behloul, D. Breysse, Characterisation of fibres distribution in a steel fibre reinforced concrete with electrical resistivity measurements, NDT & E Int. 41 (8) (2008) 638–647.
[34] W. Morris, E.I. Moreno, A.A. Sagüés, Practical evaluation of resistivity of concrete in test cylinders using a Wenner array probe, Cem. Concr. Res. 26 (12) (1996) 1779–1787.

[35] C.-T. Chen, J.-J. Chang, W-c. Yeih, The effects of specimen parameters on the resistivity of concrete, Constr. Build. Mater. 71 (2014) 35–43.
[36] A.B.L. Coppola, F. Corazza, Electrical properties of carbon nanotubes cement composites for monitoring stress conditions in concrete structures, Appl. Mech. Mater. 82 (2016) 118–123.
[37] J. Cao, D.D.L. Chung, Improving the dispersion of steel fibers in cement mortar by the addition of silane, Cem. Concr. Res. 31 (2) (2001) 309–311.
[38] I.K. Tragazikis, K.G. Dassios, D.A. Exarchos, P.T. Dalla, T.E. Matikas, Acoustic emission investigation of the mechanical performance of nano-modified mortars, Constr. Build. Mater. 122 (2016) 518–524.
[39] K.G. Dassios, P. Alafogianni, S.K. Antiohos, C. Leptokaridis, N.M. Barkoula, T.E. Matikas, Optimization of sonication parameters for homogeneous surfactant-assisted dispersion of multiwalled carbon nanotubes in aqueous solutions, J. Phys. Chem. C 119 (13) (2015) 7506–7516.